

---

# Mechanical and Thermal Properties of Dragline Silk from the Spider *Nephila clavipes*

Philip M. Cunniff<sup>1</sup>, Stephen A. Fossey<sup>1</sup>, Margaret A. Auerbach<sup>1</sup>, John W. Song<sup>1</sup>, David L. Kaplan<sup>1\*</sup>, W. Wade Adams<sup>2</sup>, Ronald K. Eby<sup>3</sup>, David Mahoney<sup>3</sup>, Deborah L. Vezie<sup>1, 2, 4</sup>

<sup>1</sup> U.S. Army Natick Research, Development & Engineering Center, Natick, Massachusetts 01760-5020, USA

<sup>2</sup> Materials Directorate, Wight Laboratory, Wright-Patterson Air Force Base, Ohio 45433-6533, USA

<sup>3</sup> Institute and Department of Polymer Science, University of Akron, Akron, Ohio 44325-3909, USA

<sup>4</sup> Department of Materials Science, MIT, Cambridge, Massachusetts 02139, USA

---

---

## ABSTRACT

Dragline silk from the spider, *Nephila clavipes*, was characterized by thermal analysis (TGA, DSC, DMA), computational modeling, scanning electron microscopy and by quasi-static as well as high rates of strain. Thermal stability to about 230°C was observed by TGA, two transitions by DMA, -75°C, representative of localized motion in the amorphous domain, and a main chain motion associated with partial melt at 210°C. Tensile tests indicated average initial modulus, ultimate tensile strength and ultimate tensile strain of 22 GPa, 1.1 GPa and 9%, respectively. The corresponding properties of the best fibers tested were 60 GPa, 2.9 GPa and 11%, respectively. High strain rates (>50,000%/sec) indicated similar mechanical properties to the average values indicated above. Microscopy showed compressive and tensile strains to failure of 34%. Computational modeling yielded a crystal modulus of 200 GPa.

**KEYWORDS:** Silk, Mechanical, Spider, Silkworm, Thermal

---

## INTRODUCTION

Materials scientists have a long-standing interest in silk fibers due to their mechanical properties, luster, dyeability, comfort and environmental stability. Historically, silkworms have been grown for silk in the Orient for thousands of years in a process known

as sericulture; spider silks have never been commercialized in this manner. In general, spider silk fibers have a unique combination of strength, stiffness and extensibility, and they generally exhibit higher strength than silkworm silk [1, 2]. The properties of silks are affected by temperature, degree of hydration and rate of deformation [2]. There have been some reports on the thermal and mechanical properties of silkworm and spider silks, with the most comprehensive set of data reported by Zemlin [1], Denny [3], Work [4] and recently by Cunniff *et al.* [5]. The crystal modulus, unit cell dimensions, compressive properties and morphology of a spider silk have been investigated recently by Mahoney *et al.* [6] and Becker *et al.* [7]. Molecular modeling of the crystal modulus for  $\beta$ -poly-L-alanine using the Tripos force field developed for synthetic polymers has been reported by Becker *et al.* [7]. The modulus value was much greater than the experimentally derived values for *Bombyx mori* and *Nephila clavipes*. The result, together with other considerations, raised questions about the validity of the assumption of uniform stress used to analyze the experimental data. In this paper we compile our recent data on the thermal and mechanical properties of silks and provide comparisons to previously published data.

Spider and silkworm silks generally consist almost entirely of protein. In silkworm cocoon silk, the fiber consists of a structural fibroin (containing two proteins, 325,000 Da and 25,000 Da) and a family of glue-like sericin proteins to hold the fibers together. Spiders produce a family of different silks,

some of which form structural parts of the orb web, while others are glue-like in function [3]. We focus here on the dragline silk, produced in the major ampullate gland and putatively consisting of one type of protein of approximately 275,000 Da [8].

Our research is focused on the elucidation of the protein content and structure of the spider silks [8, 9], molecular modeling of the protein conformations in the silk [10, 11], characterization of the liquid crystalline phases of the spider silk protein [12], membrane properties [13] and elucidation of the genetic controls involved in silk biosynthesis [14–16]. One goal of the program is to generate larger-scale production processes for these proteins for a variety of applications, including fibers, membranes and composites.

For the studies reported here, dragline silk was collected under controlled silking conditions from the major ampullate gland located in the abdomen of the spider, *N. clavipes*. This spider and silk were chosen based on Zemlin's [1] data wherein this silk generally afforded the highest strength of the silks examined.

## EXPERIMENTAL

### Organism

Specimens of the spider *N. clavipes* were used in all experiments. Female spiders were obtained from either Panama or southern Florida, USA, and housed in plexiglass enclosures until silked. Spiders were fed either crickets or nutrient solution.

### Controlled Silking

Controlled silking was performed as reported by Zemlin [1] and Work and Emerson [17] at silking rates of 1.1, 1.5, 3.1, 6.1 and 12.2 cm/sec. Spiders were not anesthetized and were placed on their dorsal side, observed with an optical microscope and the appropriate fiber teased out of the spinneret of the major ampullate gland in the abdomen. The fiber end was extracted using forceps and wound around a motorized spindle which was then continuously rotated to collect silk at constant speed. Microgram amounts of silk were collected during one silking. The spiders were returned to their enclosures for subsequent silking at a later date.

### Scanning Electron Microscopy

Samples were mounted on sample stubs with double faced adhesive tape, coated with about 30 nm of AuPd at a 72 mm working distance using 15 mA current in a sputter coater (Blazers SCD040), and viewed in a scanning electron microscope (SEM) (Amray 1000 A). Fiber diameters were measured using the image acquisition and processing program on a Noran TN-5500 X-ray analyzer. SEM photomicrographs were taken at working distances of 12–15 mm using an electron beam acceleration potential of 10 kV. Other samples for low-voltage, high-resolution scanning electron microscopy (LVHRSEM) were sputter coated with AuPd in a

Hummer X coater for 30 sec, depositing approximately a 50 Å coat. The samples were imaged using a high-resolution Hitachi S-900 field emission, immersion lens SEM at 1.0 KV.

### Thermogravimetric Analysis (TGA), Dynamic Mechanical Analysis (DMA) and Thermal Mechanical Analysis (TMA)

TGA was performed on TA Instruments TA model 2950 instrument. Test conditions included a temperature range of 25–1000°C at a heating rate of 10°C/min. Yarns of 82.3 denier, 7 mm long and 0.007 mm<sup>2</sup> cross-sectional area, were characterized on a Dynamic Mechanical Analyzer (Seiko; DMS210). Test conditions included an initial axial load applied of 200 g, a fixed frequency of 1 Hz, a temperature range of –150°C to 220°C and a heating rate of 4°C/min. Creep behavior was characterized with the same yarns using a Thermal Mechanical Analyzer (TMA) (TA Instruments). Yarn gauge length was about 2.54 cm. Test conditions included a constant stress of one newton (102 g force) and four different temperatures (–40, 25, 100 and 150°C).

### Tensile Testing

Single fibers were attached to paper tabs using an epoxy adhesive (Scotch-Weld® 1838, 3M) and cured for 24 hr; they were mounted between pneumatic fiber grips in an Instron (Model 4201), and the edges of the paper were cut off. The fiber gauge length was 5.08 cm. Each sample was examined with an optical microscope (320×) to make sure only single fibers were tested. Strain rate was 10%/sec and approximately 30 samples were tested for each type of fiber. All tests were carried out at approximately 21°C and 50% relative humidity.

### Dynamic High Strain Rate Properties

Single yarn impact tests were conducted with approximately 75 denier (linear density of a fiber, 1 denier = 1 g/9000 m) yarns collected from five to eight spiders concurrently silked. The 29.48 cm gauge length yarns were twisted approximately 1 turn/cm and clamped between rigid supports in a ballistic impact test range. The yarns were impacted transversely at the center by a 1.1 g steel projectile propelled by a compressed helium charge. Multiple microflash photography of the impact was obtained at approximately 35 μs intervals; the projectile velocity was determined before and after impact. A striking velocity of about 300 m/sec was used in each of four impact tests conducted. The photographs were digitized using an Apunix digitizer and analyzed in combination with available numerical models [18, 19].

### Computational Modeling

Silicon Graphics computers were used with the Sybyl 5.5 software from Tripos Associates, Inc. The biopolymer module and the Sybyl version of the protein-based Kollman force field [20] were used

with an array of 19  $\beta$ -poly-L-alanine molecules each containing 10 residues. Alanine was chosen since *N. clavipes* is in Warwicker's group 3b [7, 21] and there is evidence that crystals from *Antheraea pernyi* [22] as well as other group 3 silks [23] have a considerable amount of alanine in their crystals. A molecule was constructed using the fractional atomic coordinates (corrected from  $\beta$ -D-alanine) of Marsh *et al.* [22]. The energy was minimized with the torsion angles constrained to preserve the  $\beta$ -pleat. The basal projection of the array constructed with the molecule in the anti-parallel arrangement is shown in Fig. 1. Various deformation protocols were applied to the array in order to obtain the energy of the central molecule as a function of strain up to  $\pm 10^{-3}$ . The second derivative of the energy with respect to the molecular length was used, together with a correction for end effects, the initial length and the basal area per molecule to obtain the crystal modulus.

## RESULTS AND DISCUSSION

TGA of the spider silk is illustrated in Fig. 2(a) and DMA of a spider silk yarn sample is illustrated in Fig. 2(b). In the TGA, the silk is stable to approximately 230°C after which there is a rapid loss in weight upon additional heating. In the DMA, curves *a* and *a'* represent the first thermal cycle with heating to approximately 180°C (and held at that temperature for about 30 min) and the second thermal cycle (curves *b* and *b'*) was carried out until complete loss of modulus at approximately 220°C. Two transitions are noted, the first at about -70°C, presumably representing localized transition in the amorphous domain, and the second at around 210°C, representing a main chain motion associated with partial melt. Young's modulus ( $E'$ ) at the room temperature region is about 20 GPa and is maintained until about

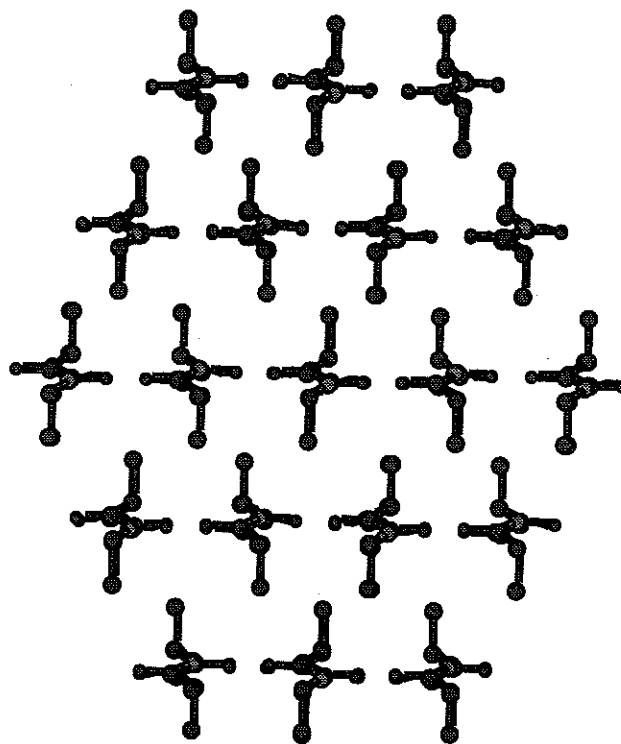


**FIGURE 1.**  $\beta$ -poly-L-alanine array composed of 19 strands of 10 residues each. The hydrogens have been removed. The side groups are directed vertically and the hydrogen bonds are directed horizontally.

170°C. The slight increase in modulus after heat treatment is presumably due to an increase in stiffness resulting from loss of moisture and increased crystallinity.

Creep compliance under a constant force of 1 N at -40, 25, 100 and 150°C indicated initial creep was strongly dependent on the initial temperature as

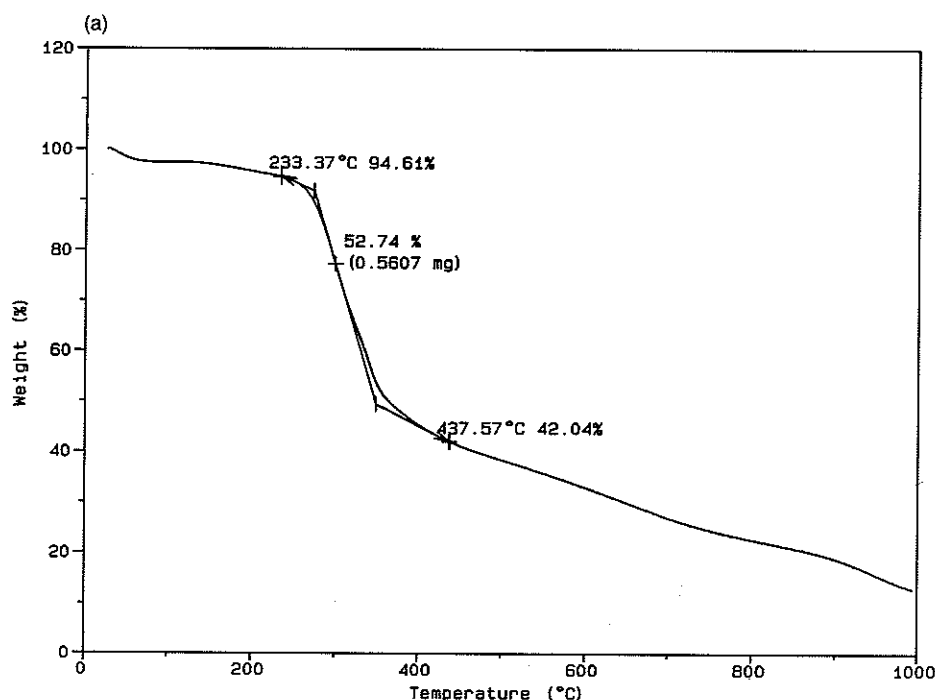


**FIGURE 2(a).** TGA scan of *N. clavipes* spider silk. A major decomposition is noted between about 230°C and 440°C.

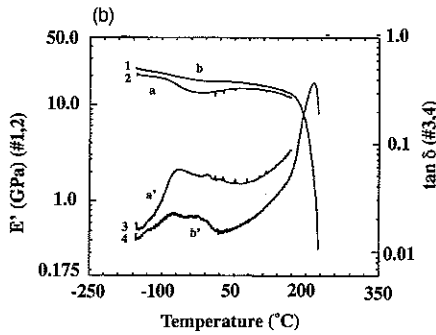


**FIGURE 2(b).** DMA scans of *N. clavipes* spider silk yarn. Curves a and a' are  $E'$  and  $\tan \delta$ , respectively, of first run. The temperature was held at 180°C for 30 min and the scan was rerun. Curves b and b' are the  $E'$  and  $\tan \delta$ , respectively, for second run on the same sample.

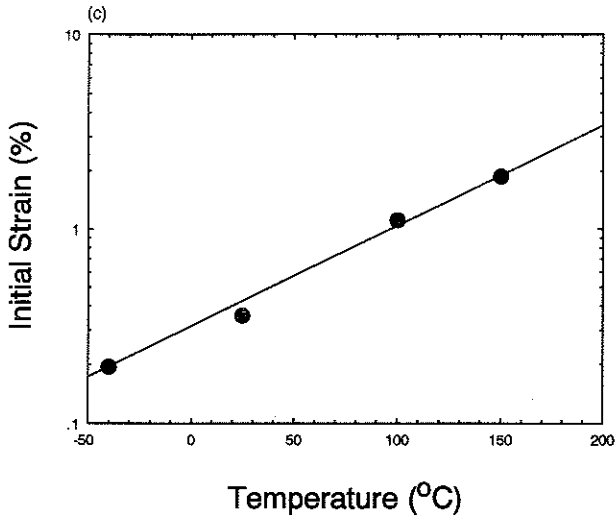


**FIGURE 2(c).** Temperature dependence of initial strain of *N. clavipes* spider silk yarn.

illustrated in Fig. 2(c). However, after the initial elongation, creep behavior was not significantly influenced by temperature, perhaps due to the extensive hydrogen bonding which may tend to limit long-term creep.

These data can be compared with previous data from the literature. Magoshi and Magoshi [24], using dynamic mechanical and dielectric properties analysis, reported a glass transition temperature,  $T_g$  of 175°C for silkworm silk (*B. mori*) using an analysis range of 20–220°C. From dielectric loss tangent measurements, they observed transition temperatures of -40°C and 175°C, with the transition at 175°C presumed to be due to crystallization. Magoshi and Nakamura [25] studied silk fibroin by DSC and reported the endotherm at 175°C due to  $T_g$  and an exotherm at 212°C due to crystallization. The exotherm at 280°C was attributed to degradation. Osaki [26] reported thermal properties of spider silks using DSC and TGA. Dragline silks from *Nephila clavata*, *Yaginumia sia* and *Argiope amoena* were characterized. An endotherm at 100°C (loss of water) and exotherms at 300, 340, 500 and 580°C (decomposition of protein) were reported for *N. clavata*. These upper values are significantly higher than those observed with the *N. clavipes* silk studied in this paper. In addition, variations in properties for the other silks were ascribed to seasonal changes.

The temperature stability of the spider silk fibers studied here, to 220°C, or the silkworm silks [24, 25, 27] would indicate suitable performance over a range of environmental conditions, particularly when compared with ultra high-molecular weight polyethylene melting temperature, ( $T_m = 147^\circ\text{C}$ ) or polyvinylalcohol fibers ( $T_m = 257^\circ\text{C}$ ) that are also considered in impact applications.

Typical single silk fibers examined by SEM indicated a regular unfractured surface with no observable gross defects as illustrated in Fig. 3, Fiber

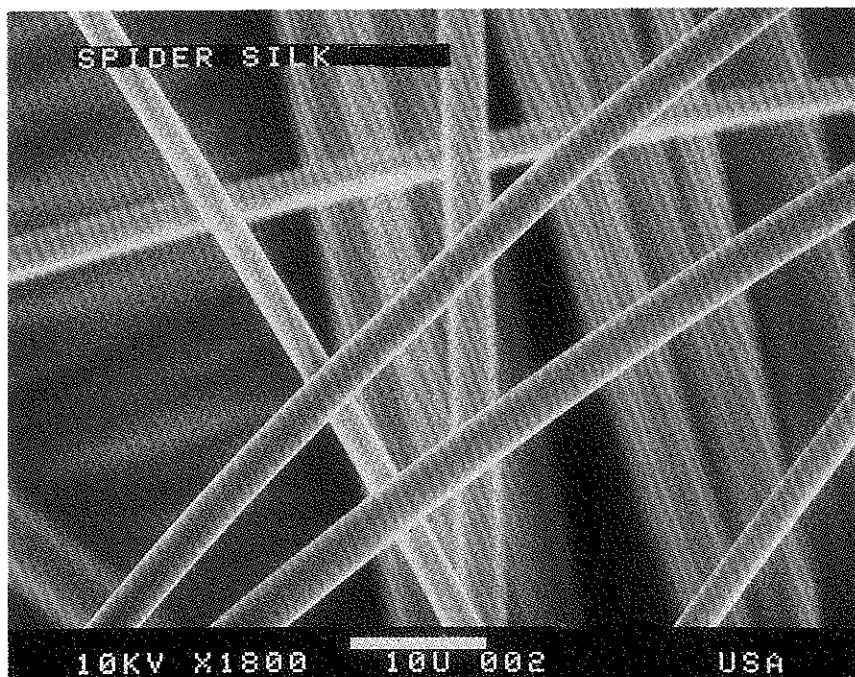


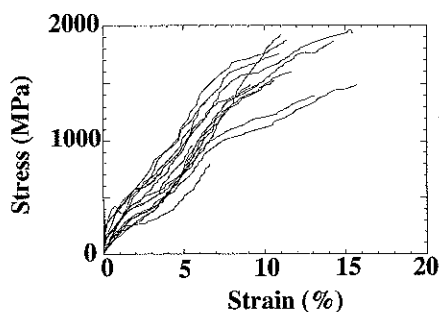
**FIGURE 3.** SEM of dragline silk fibers (1800×).

**TABLE 1.** Spider Silk Fiber Diameters as a Function of Silking Rate

Draw speed (cm/sec)	Mean diameter ( $\mu\text{m}$ )	Minimum diameter ( $\mu\text{m}$ )	Maximum diameter ( $\mu\text{m}$ )
1.5	2.45	2.19	3.01
3.1	4.49	3.97	4.85
6.1	3.60	2.23	5.36
12.2	4.31	2.95	6.29

diameters averaged  $3.0 \mu\text{m} \pm 0.62 \mu\text{m}$ . A few fibers examined showed irregularly spaced asymmetrical lobes on the surface, causing variations in the fiber diameter. This was perhaps an artifact of the silking process or fluctuations in geometry of the spinneret. Fiber diameters were determined by taking 5–18 measurements along the length of a single fiber. The data are summarized in Table 1. In all cases, a circular cross-section is assumed for the calculation of fiber cross-sectional area as previously suggested [1]. A large number of test specimens were used for subsequent stress measurements to avoid significant errors due to the use of numerical mean fiber diameters in determining cross-sectional area.

For the stress–strain data, a single fiber diameter was assumed although we recognized that there is a distribution of diameter among different fibers and some variation along a single fiber. The effect of variations on the calculation of stress cancels out when the response is averaged, assuming a Gaussian distribution about the mean. In separate studies it was concluded that the variation measured in one lot (one silking session) of fiber (Fig. 4) is representative of variability from lot to lot at the same fiber silking rate [5]. Table 2 presents the stress–strain data for silks collected at different silking rates, from 1.5 cm/sec (slightly higher than natural rates of silk spinning during orb web formation) to 12.2 cm/sec. There is

**FIGURE 4.** Variation in stress–strain response of single fibers.

no obvious correlation between silking rate and mechanical properties evident from the data. In addition, Table 3 summarizes the stress–strain data for quasi-static testing and high strain testing of the fibers. Quasi-static stress–strain tests allow stress relaxation or creep, while at the high strain rates times are usually too short for appreciable chain motion to occur. A detailed description of the methods of calculation and interpretation of the high strain rate data are reported elsewhere [5].

Figure 5 shows a LVHRSEM image of one fiber bent sharply around another. A simplified calculation shows the strains to be approximately 34% in tension and compression on the outer and inner surfaces of the bend, respectively. These approach the upper limits of the reported strains for tension [28] and compression [6]. In Fig. 5, there is no evidence of tensile breaking at the outer surface of the bend. In Fig. 6, which shows the bend at higher magnification, there is no evidence of failure by kinking at the inner compressive surface of the fiber. Synthetic high-performance fibers exhibit kinking under these experimental conditions. The lack of kinking is consistent with either the absence of microfibrils or the presence of microfibrils which exhibit strong lateral interactions [29].

Significant variability is observed in determining the mechanical properties of the silks. This may in part be due to gross defects causing fiber failure, or inaccurate fiber diameter used to calculate stress. Since the strength of a given fiber is determined by the minimum cross-section present in the test sample, both factors may be significant in these variations. Fracture topography for the 10%/sec strain rate was typically rough, indicative of ductile fracture, with no gross defects as illustrated in Fig. 7. Fibers strained to break in less than 200  $\mu\text{s}$  at a strain rate in excess of 50,000%/sec exhibited similar fracture surfaces to those under quasi-static conditions. Infrequent and limited fibrillation was observed in some fibers.

Computational modeling yielded a crystal modulus of 200 GPa. The value determined with the force

**TABLE 2.** Stress–Strain Data for Silks Collected at Different Silking Rates

Silking rate (cm/sec)	Initial modulus (GPa)	Secant modulus (GPa)	Ultimate tensile strength (GPa)	Ultimate tensile strain (%)
1.5	35.0	16.0	1.7	10.7
3.1	20.2	11.0	0.7	7.7
6.1	35.0	21.1	1.3	6.0
12.2	19.5	9.7	1.2	12.2

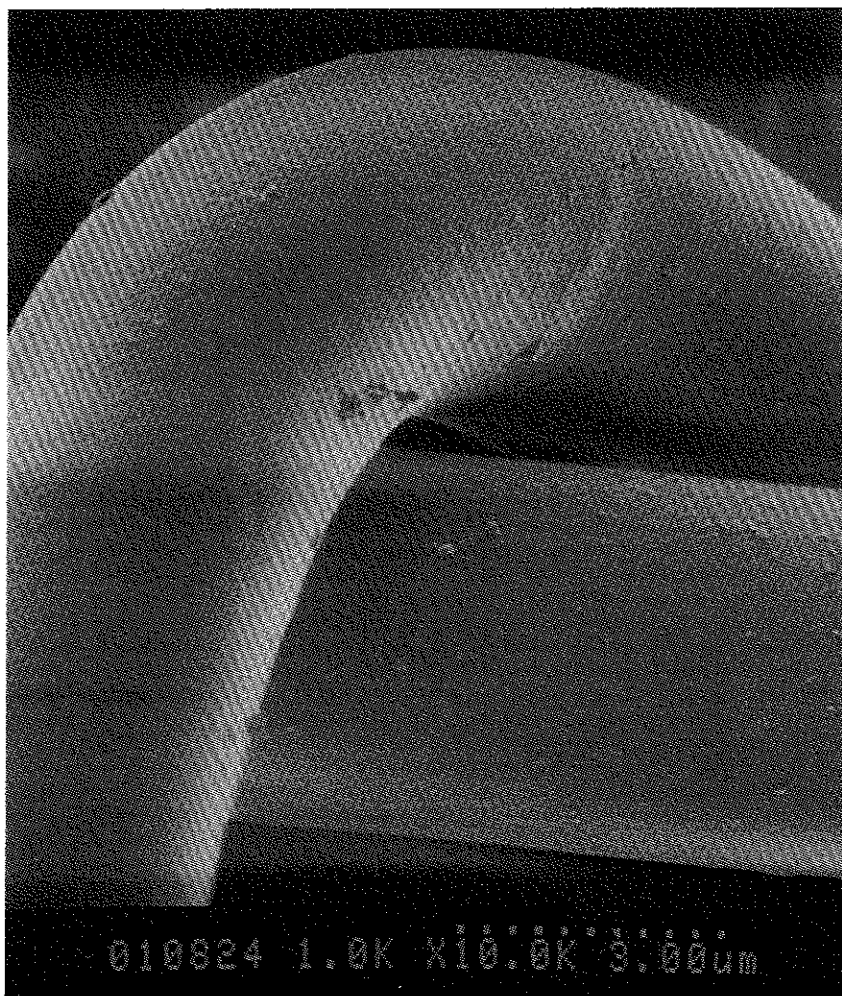
**TABLE 3.** Summary of Mechanical Properties of Spider Silk (gpd = grams per denier)

Property	Quasi-static (average)	Quasi-static (high end)	High strain
Initial modulus	22 GPa (190 gpd)	60 GPa (500 gpd)	20 GPa (175 gpd)
Secant modulus	13 GPa (109 gpd)	25 GPa (208 gpd)	10 GPa (85 gpd)
Ultimate tensile strength	1.1 GPa (10 gpd)	2.9 GPa (24 gpd)	—
Ultimate tensile strain	9%	11%	10%

field for synthetic polymers was about 25% smaller [7]. The new value can be considered to be the better one since it was determined with a protein-based force field. Both values are much greater than the experimental values of 17 GPa for *N. clavipes* and 29 GPa for *B. mori* reported by Becker et al. [7]. Results obtained from Treloar's method, 155 GPa, for *B. mori* [30] and from the slope of the longitudinal acoustic dispersion curve, 147 GPa, calculated for  $\beta$ -poly-L-glycine with a modified Urey-Bradley force field [31] are also greater than the experimental values. These results raise a question about the validity of the

proposed use of the assumption of uniform stress in the analysis of the experimental data [32].

Prior data on the mechanical properties of silks in the literature are summarized here. Zemlin [1] reported the mechanical properties of spider silks (both web silks and silks obtained under controlled silking conditions) for spiders collected in Brazil and Florida; (*N. clavipes*, *Argiope aurantia*, *Nephila cruentata*, *Parawixla audax*, *Argiope argentata*). Controlled silking was the primary approach used to generate useful materials for determinations of mechanical performance. Silking rates were 1.9–61 cm/sec

**FIGURE 5.** LVHRSEM of one *N. clavipes* fiber bent around another.

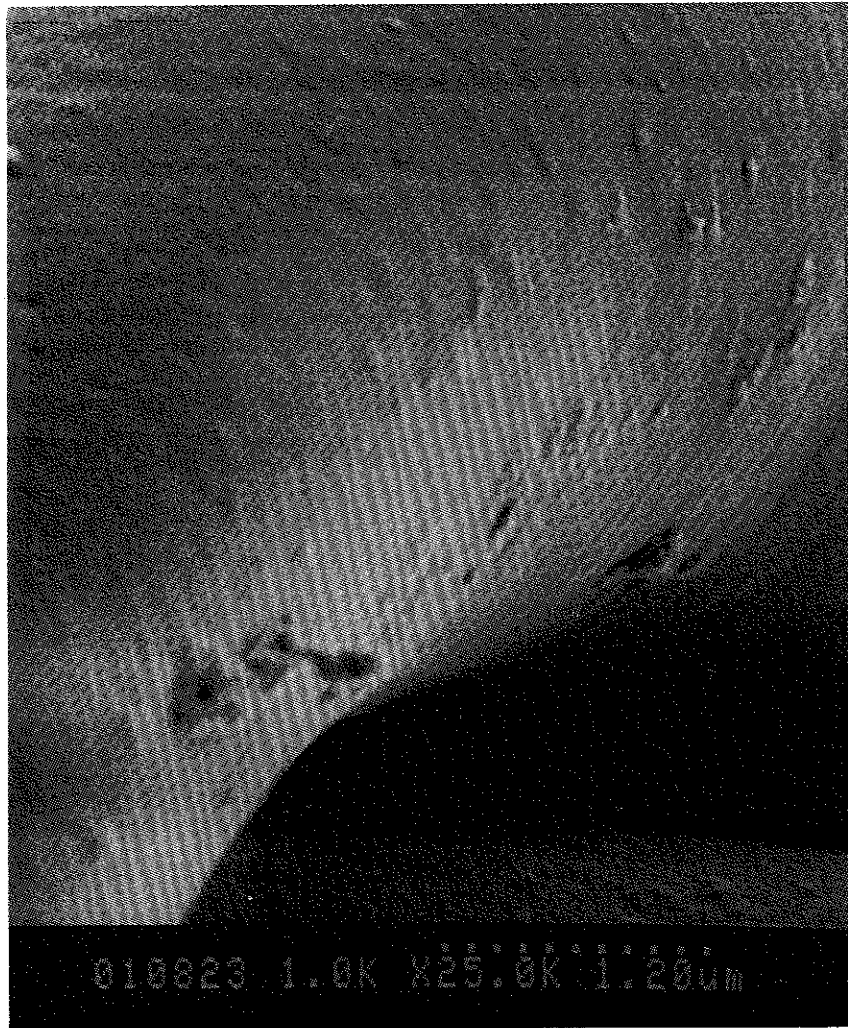


**FIGURE 6.** Higher magnification image of the compressive side of the bent fiber from Fig. 5.

**TABLE 4.** Summary of Spider Silk Mechanical Data collected by Zemlin (1969) (Top) and Reported By Calvert (1988) (Bottom). Calculated from Data in the References

Spider species	Controlled silking (C) Natural silk (N)	Tenacity (MPa)	Elongation (%)	Initial modulus (GPa)
<b>Spiders</b>				
<i>Nephila clavipes</i>	C	972	18.1	12.7
	N	875	16.7	10.9
<i>Argiope aurantia</i>	C	1350	20.0	9.7
	N	798	20.6	9.9
<i>Nephila cruentata</i>	N	505	19.9	3.6
<i>Parawixla audax</i>	N	504	21.2	3.1
<i>Argiope argentata</i>	N	436	17.2	4.0
Maximum values	C/N	2042	39.7	31.8
<b>Silkworm</b>				
<i>Bombyx mori</i>	N	740	20	10
<b>Spiders</b>				
<i>Araneus diadematus</i>				
dragline	N	1190	31	2.8
cocoon	N	360	46	0.6
sticky spiral	N	-	517	-



**FIGURE 7.** Fracture topography of dragline silk at 10%/sec strain rate.

(natural silk spinning rates are around 1 cm/sec) and mechanical testing was performed at 65% RH, 70°C and 100%/min strain rate. Fibers ranged in diameter from 1 to 8  $\mu\text{m}$  depending on the type and source of silk. Table 4 was compiled from the original report and summarizes the data from that study. Zemlin [1] also found that the mechanical properties generally decreased with increasing silking rate from 1.9 to 61 cm/sec for *N. clavipes*. Some of these rates were considerably higher than the rates used in the study reported here. Zemlin [1] had indicated that higher-strength fibers were obtained at lower silking rates, although the modulus and extension to break were not changed. Also, larger diameter fibers were observed at higher silking rates with additional damage noted to the fibers.

Work [4] summarized much of the early studies on mechanical properties of various spider silks, including Herzog, who first reported the mechanical strength of cocoon silk from the spider *Nephila madagascariensis* at 0.41 GPa, DeWilde, who reported the strength properties of frame silk from *Araneus diadematus* at 1.39 GPa and 25–30% elongation to break, and Lucas, who found 0.95 GPa strength and 31% elongation to break for fibers from *A. diadematus*. Work [4] reported 1.1 GPa strength and 35% elongation in studies on fibers from the spiders *Euriophora fuligenia*, *A. argentata*, *A. diadematus*, *N. clavipes* and *A. aurantia*. He also indicated that spiders completely anesthetized under carbon dioxide produce fibers of poorer quality (lower strength). Data reported by Calvert [33] are also summarized in Table 4 for comparison.

Denny [3] conducted an extensive study of viscid (circular stands on an orb web produced in the flagelliform gland and coated with a layer of glue produced in the aggregate gland) and frame silks

(radial strands in the orb web produced in the major ampullate gland, which may be multiple strands; the major ampullate gland also produces the dragline silk) from webs of *Araneus sericatus*. Samples were 1–3  $\mu\text{m}$  in diameter and samples were stored at ambient temperature and humidity. He reported a strength of 1 GPa. He concluded that viscid silks were elastic materials functioning as shock absorbers and the frame silks were viscoelastic materials functioning as structural elements in the orb web aerial filter.

Work and coworkers [34, 35] reported that dragline silk from *N. cruentata*, when axially unrestrained, can supercontract up to 55% of the original length. This same feature was not observed with minor ampullate gland silk or silkworm silk. Gosline *et al.* [36] proposed that the dragline silk of *A. diadematus* could be considered a rubber, with the amorphous regions providing an energy-absorbing matrix containing inclusions of the stiffer crystalline domains. Vollrath and Edmonds [37] reported that a key difference between radial and capture threads of *A. diadematus* was due to a water coating on capture threads which plasticize the material and enhance elasticity.

Gosline *et al.* [2] reviewed the available data on mechanical properties of spider silks which dissipate energy of impact (flying insects) without breaking. Silkworm silks are primarily formed as a barrier against environmental stresses during molting, while the spider silks provide a major mechanical function of an orb web. For example, they reported that a 75 mg spider uses 180  $\mu\text{g}$  of protein to produce an orb web sufficient to collect its food for survival. They reported frame silk exhibits an initial modulus of 10 GPa which drops to 4 GPa in the final linear region of the curve. The maximum strength was

1.4 GPa. The silkworm (*B. mori*) exhibits the same initial stiffness, a strength of 0.7 GPa and 20% extension to break [2]. This information allowed them to calculate a measure of energy to break of  $1.5 \times 10^5$  J/kg. Based on their calculations, 70% of the energy of impact is dissipated as heat through viscoelastic processes. This means the energy is not available for elastic recoil and the captured prey stays in the web instead of being jettisoned, and the integrity of the web is maintained without breaking. Hysteresis contributes to high strength and toughness of the material.

Gosline *et al.* [2] also noted that viscid silk can exhibit 200% extension and low stiffness, with an initial modulus of 3 MPa which rises to 500 MPa at large extensions to break. Therefore low stiffness and high extensibility match the function of the silk because the captured insect cannot get out as there is nothing stiff enough to hold on to [2]. They also report a volume fraction of crystalline material of 30% [2], although recently Thiel *et al.* [38] reported this may be as high as 50%. Iizuka [39] reported on the mechanical properties of six different races of silkworm silk (*B. mori*) and found 160 GPa as the theoretical limit of elastic modulus for a crystal of silk fibroin. This value compares favorably with the theoretical elastic limit for poly L-alanine (160 GPa) and poly L-glutamine (230 GPa) in the extended chain form [40], as well as with the crystal modulus for  $\beta$ -poly-L-alanine computed previously (150 GPa) and in this article (200 GPa). Laible [41] investigated the high strain rate properties of a number of polymeric fibers including silkworm silk. He reported a ballistic limit value of 426 m/sec for silkworm silk, as compared to 500 m/sec for Kevlar 29 and 380 m/sec for nylon. The relatively high ballistic limit, despite poorer quasi-static properties, for silkworm silk was speculated to be related to a high elongation to break at a very high strain rate.

Recently, Lock [42] has reported the successful solubilization and re-spinning of silkworm silk into fibers with mechanical properties comparable to the native fiber. The approach was to solubilize the silk fibroin in LiSCN at 5–40 wt%, dialyze, lyophilize or evaporate the water, and then resolubilize in hexafluoroisopropanol. A solution of 5–25 wt% could be spun. The advantage here is the ability to control fiber diameter and different flow rates with new opportunities for the study of mechanical properties.

The data reported in the present study indicate mechanical properties of spider silks are unusual, with a unique combination of strength, stiffness and elongation. In addition, the data reported here for high strain rates indicate similar mechanical behavior as found in quasi-static tests. The data also show that the dragline silk of *N. clavipes* exhibits tensile and compressive elongations to failure that are superior to those of high-performance synthetic fibers. The crystal modulus for  $\beta$ -poly-L-alanine computed with a protein-based force field is 200 GPa. This value is comparable to those for a number of synthetic fibers. It is 7–12 times the experimental values for the silks. These data indicate useful ranges of thermal stability, as well as potentially important

mechanical performance for fiber and composite applications.

## ACKNOWLEDGEMENTS

Portions of this work were supported by a contract with Lawrence Associates, Inc, and by Tripos Associates Inc.

## REFERENCES

1. J. C. Zemlin, Technical Report TR69-29-CM (AD684333), US Army Natick Laboratories, Natick, Massachusetts (1968).
2. J. M. Gosline, M. E. DeMont and M. W. Denny, *Endeavor*, 10, 37 (1986).
3. M. Denny, *J. Exp. Biol.*, 65, 483 (1976).
4. R. W. Work, *Text. Res. J.*, 7, 485 (1976).
5. P. M. Cunniff, S. A. Fossey, M. A. Auerbach and J. W. Song, *Silk Polymers: Materials Science and Biotechnology* (D. L. Kaplan, W. W. Adams, B. Farmer, C. Viney, eds), ACS Symp. Series 544 (1993).
6. D. V. Mahoney, D. L. Vezie, R. K. Eby, W. W. Adams and D. L. Kaplan, *Silk Polymers: Materials Science and Biotechnology* (D. L. Kaplan, W. W. Adams, B. Farmer and C. Viney, eds), ACS Symp. Series 544 (1993).
7. M. A. Becker, D. V. Mahoney, P. G. Lenhart, R. K. Eby, D. L. Kaplan and W. W. Adams, *Silk Polymers: Materials Science and Biotechnology* (D. L. Kaplan, W. W. Adams, B. Farmer, C. Viney, eds), ACS Symp. Series 544 (1993).
8. C. M. Mello, K. Senecal, B. Yeung, P. Vouros and D. L. Kaplan, in *Silk Polymers: Materials Science and Biotechnology* (D. L. Kaplan, W. W. Adams, B. Farmer, C. Viney, eds), ACS Symp. Series 544 (1993).
9. S. J. Lombardi and D. L. Kaplan, *Polym. Prep. Am. Chem. Soc.*, 31, 195 (1990).
10. S. A. Fossey, G. Nemethy, K. D. Gibson and H. A. Scheraga, *Biopolymers*, 31, 1529 (1991).
11. S. A. Fossey and D. L. Kaplan, *Silk Polymers: Materials Science and Biotechnology* (D. L. Kaplan, W. W. Adams, B. Farmer, C. Viney, eds), ACS Symp. Series 544 (1993).
12. K. Kerkam, C. Viney, D. L. Kaplan and S. Lombardi, *Nature*, 349, 596 (1991).
13. W. S. Muller, L. A. Samuelson, S. A. Fossey and D. L. Kaplan, *Langmuir*, 9, 1857 (1993).
14. S. J. Lombardi and D. L. Kaplan, *J. Arachnol.*, 18, 297 (1990).
15. S. J. Lombardi and D. L. Kaplan, *Acta Zool. Fennica*, 190, 243 (1990).
16. R. Beckwitt and S. Arcidiacono, *J. Biol. Chem.*, 269, 6661 (1994).
17. R. W. Work and P. D. Emerson, *J. Arachnol.*, 10, 1 (1982).
18. D. K. Roylance, *J. Appl. Mech.*, 143, 148 (1973).
19. P. M. Cunniff, US Army Symposium on Solid Mechanics, Newport, RI (1989).
20. S. J. Weiner, P. A. Kollman, D. A. Case, U. C. Singh, C. Ghio, G. Alagona, S. Profeta Jr and P. J. Weiner, *Am. Chem. Soc.*, 106, 765 (1984).
21. J. O. Warwicker, *J. Mol. Biol.*, 2, 350 (1960).
22. R. E. Marsh, R. B. Corey and L. Pauling, *Acta Cryst.*, 8, 710 (1955).
23. J. T. B. Shaw and S. G. Smith, *Biochim. Biophys. Acta*, 52, 305 (1961).
24. J. Magoshi and Y. Magoshi, *J. Polym. Sci.*, 13, 1347 (1975).
25. J. Magoshi and S. Nakamura, *J. Appl. Polym. Sci.*, 19, 1013 (1975).
26. S. Osaki, *Acta Arachnol.*, 37, 69 (1989).

27. S. Nakamura, J. Magoshi and Y. Magoshi, in *Silk Polymers: Materials Science and Biotechnology* (D. L. Kaplan, W. W. Adams, B. Farmer, C. Viney, eds), ACS Symp. Series 544 (1993).
28. G. A. M. Butterworth and R. W. Lenz, Report C65593 to US Army Natick Laboratories; Fabric Research Laboratories Inc., Dedham, MA, May (1966).
29. D. L. Vezie, PhD Dissertation, MIT (1993).
30. E. Iizuka, *Biorheology*, 3, 1 (1965).
31. B. M. Franconi, *Chem. Phys.*, 57, 2109 (1972).
32. K. Nakamae, J. Nishino and H. Ohkubo, *Polymer*, 30, 1243 (1989).
33. P. D. Calvert, *Encyclopedia Materials Sci. Eng., Biological Macromolecules*, Pergamon Press, pp. 334 (1988).
34. R. W. Work and N. Morosoff, *Tex. Res. J.*, 5, 349 (1982).
35. R. W. Work, *J. Exp. Biol.*, 118, 379 (1985).
36. J. M. Gosline, M. W. Denny and M. E. DeMont, *Nature*, 309, 551 (1984).
37. F. Vollrath and D. T. Edmonds, *Nature*, 340, 305 (1989).
38. B. Thiel, D. Kunkel, K. Guess and C. Viney, *Materials Research Society Symp.*, Vol. 330, in press.
39. E. Iizuka, *J. Appl. Polymer Sci.*, 41, 173 (1985).
40. R. Pachter, R. L. Crane and W. W. Adams, *Polymers: Materials Science and Biotechnology* (D. L. Kaplan, W. W. Adams, B. Farmer, C. Viney, eds), ACS Symp. Series 544 (1993).
41. R. C. Laible, Fibrous armor in *Ballistic Materials and Penetration* (S. P. Wolsky and A. W. Czanderno, eds), Elsevier (1980).
42. R. Lock, PCT Patent W093/15244 (1993).